



## ApoA-I mimetic peptides promote pre- $\beta$ HDL formation in vivo causing remodeling of HDL and triglyceride accumulation at higher dose

Ester Carballo-Jane<sup>a,\*</sup>, Zhu Chen<sup>a</sup>, Edward O'Neill<sup>a</sup>, Jun Wang<sup>a</sup>, Charlotte Burton<sup>a</sup>, Ching H. Chang<sup>a</sup>, Xun Chen<sup>a</sup>, Suzanne Eveland<sup>a</sup>, Betsy Frantz-Wattley<sup>a</sup>, Karen Gagen<sup>a</sup>, Brian Hubbard<sup>a</sup>, Marina Ichetovkin<sup>a</sup>, Silvi Luell<sup>a</sup>, Roger Meurer<sup>a</sup>, Xuelei Song<sup>a</sup>, Alison Strack<sup>a</sup>, Annunziata Langella<sup>b</sup>, Simona Cianetti<sup>b</sup>, Francesca Rech<sup>b</sup>, Elena Capitò<sup>b</sup>, Simone Bufali<sup>b</sup>, Maria Veneziano<sup>b</sup>, Maria Verdirame<sup>b</sup>, Fabio Bonelli<sup>b</sup>, Edith Monteagudo<sup>b</sup>, Antonello Pessi<sup>b</sup>, Raffaele Ingenito<sup>b</sup>, Elisabetta Bianchi<sup>b,\*</sup>

<sup>a</sup>Merck Research Laboratories, 126 East Lincoln Avenue, RY80Y-140, Rahway, NJ 07065, USA

<sup>b</sup>Merck Research Laboratories, Istituto di Ricerche di Biologia Molecolare P. Angeletti, 00040 Pomezia, Rome, Italy

### ARTICLE INFO

#### Article history:

Received 28 July 2010

Revised 20 September 2010

Accepted 21 September 2010

Available online 4 November 2010

#### Keywords:

Peptide mimetics

ApoA-I

HDL (high density lipoproteins)

Pre- $\beta$  HDL

Atherosclerosis

### ABSTRACT

Reverse cholesterol transport promoted by HDL-apoA-I is an important mechanism of protection against atherosclerosis. We have previously identified apoA-I mimetic peptides by synthesizing analogs of the 22 amino acid apoA-I consensus sequence (apoA-I<sub>cons</sub>) containing non-natural aliphatic amino acids. Here we examined the effect of different aliphatic non-natural amino acids on the structure–activity relationship (SAR) of apoA-I mimetic peptides. These novel apoA-I mimetics, with long hydrocarbon chain (C<sub>5–8</sub>) amino acids incorporated in the amphipathic  $\alpha$  helix of the apoA-I<sub>cons</sub>, have the following properties: (i) they stimulate in vitro cholesterol efflux from macrophages via ABCA1; (ii) they associate with HDL and cause formation of pre- $\beta$  HDL particles when incubated with human and mouse plasma; (iii) they associate with HDL and induce pre- $\beta$  HDL formation in vivo, with a corresponding increase in ABCA1-dependent cholesterol efflux capacity ex vivo; (iv) at high dose they associate with VLDL and induce hypertriglyceridemia in mice. These results suggest our peptide design confers activities that are potentially anti-atherogenic. However a dosing regimen which maximizes their therapeutic properties while minimizing adverse effects needs to be established.

© 2010 Elsevier Ltd. All rights reserved.

### 1. Introduction

Many factors may contribute to the ability of HDL, or its main protein constituent, apoA-I, to protect against atherosclerosis. One of the primary mechanisms of atheroprotection is believed to be reverse cholesterol transport (RCT), the process of cholesterol efflux from arterial macrophages to HDL resulting in delivery of excess cholesterol to the liver for excretion in bile and ultimate elimination in feces.<sup>1,2</sup>

RCT is a regulated process mediated by specific transporters.<sup>3</sup> In particular, the ATP-binding cassette transporter A1 (ABCA1) is believed to initiate the process, by mediating cholesterol efflux from macrophages to lipid-free or lipid-poor apoA-I,<sup>4</sup> generating nascent HDL particles. Many studies have documented the anti-atherogenic effects of apoA-I in animal models.<sup>5,6</sup> These observations highlight the therapeutic potential of apoA-I-based treatments,

including infusion of apoA-I itself, and pharmacological agents that upregulate apoA-I expression.<sup>7,8</sup> Here we focus on another approach, the development of apoA-I mimetic peptides that recapitulate certain pharmacological features of apoA-I while being easier and less expensive to manufacture.

Despite the importance of ABCA1 in nascent HDL biogenesis and atheroprotection, relatively little is known about the structural elements of apoA-I that mediate ABCA1-dependent cholesterol efflux. ApoA-I is a 243 amino acid protein containing multiple  $\alpha$ -helical repeats separated by proline residues. Most of the repeats are 22 amino acids long with a unique secondary structure defined as class A amphipathic  $\alpha$ -helix. In this helix, negatively charged amino acid residues are clustered at the center of the polar face and positively charged residues are at the interface between the hydrophilic and hydrophobic faces. The apoA-I segments that have been implicated in mediating cellular lipid efflux are those that possess the highest lipid binding affinity.<sup>9,10</sup>

Although individual 22-mer helices of apoA-I are incapable of stimulating ABCA1-dependent cholesterol efflux, longer peptides consisting of more than one repeat are able to promote cholesterol efflux.<sup>9</sup> In addition, a variety of peptides unrelated to apoA-I but

\* Corresponding authors. Tel.: +1 732 594 8489 (E.C.-J.); tel.: +39 06 91093434 (E.B.).

E-mail addresses: [ester\\_carballojane@merck.com](mailto:ester_carballojane@merck.com) (E. Carballo-Jane), [e.bianchi@irbm.it](mailto:e.bianchi@irbm.it) (E. Bianchi).

with amphipathic helical characteristics have been shown to promote cholesterol efflux from cells and to mimic additional activities of apoA-I, such as anti-oxidation and anti-inflammation.<sup>11–14</sup> In particular, the apoA-I mimetic peptide D4F was reported to have anti-atherogenic effects in animal models.<sup>15,16</sup>

We have previously discovered that starting from an inactive 22-mer consensus sequence of the tandem repeats of apoA-I (apoA-I<sub>cons</sub>)<sup>17</sup> it was possible to design apoA-I mimetic peptides that could: i) mediate cholesterol efflux via ABCA1 from macrophages in vitro, and ii) cause an increase in pre- $\beta$  HDL formation in vitro when incubated with both human and mouse plasma.<sup>18</sup> Key to the activity of these peptides was increased lipophilicity of the peptides achieved by introducing alkenyl long hydrocarbon chain amino acids into the sequence, resulting in the formation of an all-hydrocarbon cycle by ring closing metathesis. The observation that the introduction of a few alkenyl amino acids per se influenced the activity of apoA-I mimetic peptides prompted us to further explore the potential of introducing a new set of aliphatic non-natural amino acids on the hydrophobic face of apoA-I<sub>cons</sub>. Here we describe the detailed structure–activity relationship (SAR) of novel peptides containing long hydrocarbon chain (C<sub>5–8</sub>) amino acids incorporated at all positions of the hydrophobic portion of the class A amphipathic  $\alpha$ -helix of apoA-I<sub>cons</sub>. We started by synthesizing a series of novel non-natural amino acids that had both alkenyl and alkanyl side chains of different configuration. We then carried out SAR studies on peptide analogs containing these non-natural amino acids. This led to the identification of specific positions at which introduction of a long hydrocarbon chain confers on the 22-mer peptide pharmacological features characteristic of apoA-I (Fig. 1). We found that novel apoA-I mimetic peptides which can stimulate in vitro cholesterol efflux from macrophages via ABCA1 also induce pre- $\beta$  HDL formation in human and mouse plasma in vitro, trigger HDL remodeling and pre- $\beta$  HDL formation upon administration into animals (with a concomitant increase in serum ABCA1-dependent cholesterol efflux

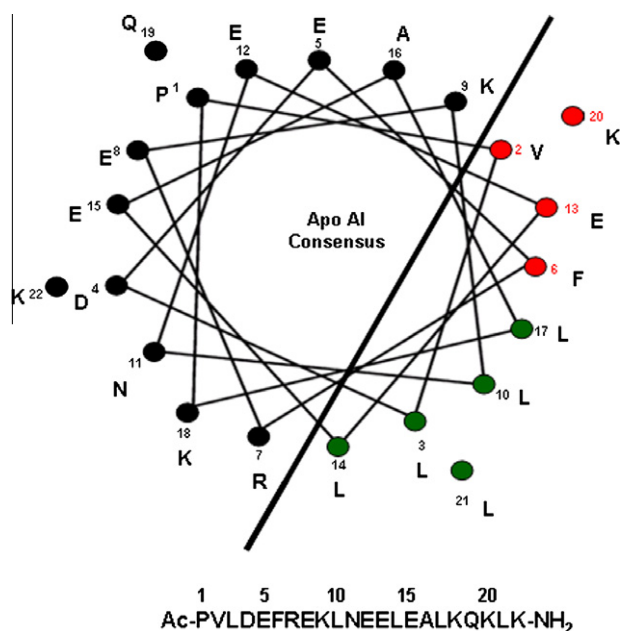


**Figure 1.** Helical wheel representation and peptide sequence of the 22-mer consensus peptide of the tandem repeats of apoA-I, apoA-I<sub>cons</sub>. The black bar highlights the interface between the hydrophilic and hydrophobic faces. Highlighted with a green or red ball are positions where aliphatic non-natural amino acids were introduced. In red are the positions identified by the SAR as most suitable for gaining activity in the cholesterol efflux assay.

**Table 1**

Single-point mutant sequence of apoA-I<sub>cons</sub>

ApoA-I <sub>cons</sub> analogs <sup>a</sup>	Sequence
ApoA-I <sub>cons</sub>	PVLDEFREKLN EEEAL KQK LK
X-2	PXLDEFREKLN EEEAL KQK LK
X-3	PVXDEFREKLN EEEAL KQK LK
X-6	PVLDEXREKLN EEEAL KQK LK
X-9	PVLDEFREXL NEE EAL KQK LK
X-10	PVLDEFREKX NEE EAL KQK LK
X-13	PVLDEFREKLN EX EAL KQK LK
X-14	PVLDEFREKLN EEX EAL KQK LK
X-17	PVLDEFREKLN EEEAL XK QK LK
X-20	PVLDEFREKLN EEEAL KQX LK
X-21	PVLDEFREKLN EEEAL KQKX K

<sup>a</sup> X represents the amino acid substitution at numbered position of apoA-I<sub>cons</sub>.

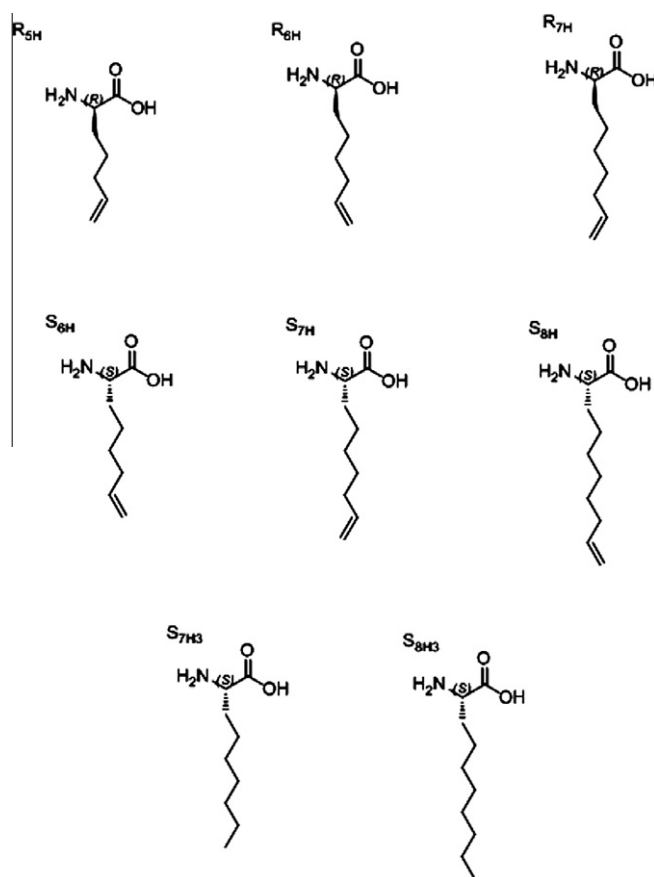


**Figure 2.** Panel of non-natural amino acids with long hydrocarbon side chains introduced for the SAR of apoA-I<sub>cons</sub> peptide.

capacity ex vivo), and, at high concentration, incorporate into VLDL and induce hypertriglyceridemia in mice.

## 2. Results and discussion

### 2.1. Design and synthesis of apoA-I<sub>cons</sub> peptide analogs

Figure 1 shows the sequence and helical wheel representation of the 22 amino acid consensus sequence, apoA-I<sub>cons</sub>, with its unique secondary structural element defined as a class A amphipathic  $\alpha$ -helix. In the helix, negatively charged amino acid residues are clustered at the center of the polar face and positively charged

residues are at the interface between the hydrophilic and hydrophobic faces. On the helical wheel of apoA-I<sub>cons</sub>, the hydrophobic face comprises residues numbered on the sequence as 2, 3, 6, 9, 10, 13, 14, 17, 20, and 21. We synthesized analogs of apoA-I<sub>cons</sub> with hydrophobic non-natural amino acids at each of these positions following the scheme shown in Table 1.

The non-natural amino acid substitutions have long carbon (C<sub>5–8</sub>) alkenyl or alkanyl side chains, in both *R* or *S* configuration, as shown in Figure 2. Our goal was to stabilize the class A  $\alpha$ -helical motif and modulate lipophilicity of the amphipathic helix. Amino acids Fmoc-R<sub>5H</sub>, Fmoc-R<sub>6H</sub> and Fmoc-S<sub>7H</sub> were synthesized as previously described,<sup>18</sup> while the synthesis of alkenyl amino acids Fmoc-S<sub>6H</sub>, Fmoc-R<sub>7H</sub>, Fmoc-S<sub>8H</sub>, and alkanyl amino acids Fmoc-S<sub>7H3</sub> and Fmoc-S<sub>8H3</sub> were described in Section 4.

The 22-mer peptide apoA-I<sub>cons</sub> analogs were synthesized by solid phase using Fmoc/Bu chemistry on a peptide synthesizer using 2-(1*H*-benzotriazole-1-yl)-1,1,3,3-tetramethyluronium hexafluorophosphate (HBTU) as coupling reagent and a Fmoc-Rink AM-PS based resin. All the experimental details are available in Section 4.3.

**Table 2**  
In vitro cholesterol efflux from macrophages

Compd No.	Name	Chol. efflux (EC <sub>50</sub> , $\mu$ M) <sup>a</sup>
1	ApoA-I <sub>cons</sub>	>100
2	D4F	2 $\pm$ 0.25
3	5A	3.4 $\pm$ 1.06
4	h-apoA-I protein	0.1 $\pm$ 0.01
5	S <sub>6H</sub> -2	>100 <sup>+</sup>
6	S <sub>6H</sub> -3	>100
7	S <sub>6H</sub> -6	>100
8	S <sub>6H</sub> -9	>100
9	S <sub>6H</sub> -10	>100
10	S <sub>6H</sub> -13	1.4
11	S <sub>6H</sub> -14	>100
12	S <sub>6H</sub> -17	>100
13	S <sub>6H</sub> -20	213
14	S <sub>6H</sub> -21	>100
15	R <sub>6H</sub> -2	>100 <sup>+</sup>
16	R <sub>6H</sub> -3	>100
17	R <sub>6H</sub> -6	>100
18	R <sub>6H</sub> -9	>100
19	R <sub>6H</sub> -10	>100
20	R <sub>6H</sub> -13	31 $\pm$ 18
21	R <sub>6H</sub> -14	>100
22	R <sub>6H</sub> -17	>100
23	R <sub>6H</sub> -20	>100 <sup>+</sup>
24	R <sub>6H</sub> -21	>100
25	R <sub>5H</sub> -6	>100
26	R <sub>5H</sub> -13	>100 <sup>+</sup>
27	S <sub>7H</sub> -6	>100 <sup>+</sup>
28	S <sub>7H</sub> -9	>100
29	S <sub>7H</sub> -10	>100
30	S <sub>7H</sub> -13	2.4 $\pm$ 0.6
31	S <sub>7H</sub> -14	>100
32	S <sub>7H</sub> -17	>100
33	S <sub>7H</sub> -20	>100 <sup>+</sup>
34	R <sub>7H</sub> -2	>100 <sup>+</sup>
35	R <sub>7H</sub> -6	>100
36	R <sub>7H</sub> -9	>100
37	R <sub>7H</sub> -10	>100
38	R <sub>7H</sub> -13	9.5 $\pm$ 3.3
39	R <sub>7H</sub> -14	>100
40	R <sub>7H</sub> -17	>100
41	R <sub>7H</sub> -20	>100
42	R <sub>7H</sub> -21	>100
43	S <sub>7H3</sub> -13	0.7 $\pm$ 0.1
44	S <sub>8H</sub> -13	0.7 $\pm$ 0.3
45	S <sub>8H3</sub> -13	0.7 $\pm$ 0.2

The activity is gained by introduction of one aliphatic non-natural amino acid at positions of apoA-I<sub>cons</sub>.

<sup>a</sup> >100<sup>+</sup>, Weakly active at the highest concentration tested.

The non-natural amino acids were coupled manually using HBTU as activator until a negative ninhydrin test was observed. All the peptides were purified by reverse-phase chromatography at purity above 95%, as determined by analytical HPLC chromatography.

After assessing the cholesterol efflux activities of each of the single substitution analogs, the substitutions in the most active analogs were combined in analogs of apoA-I<sub>cons</sub> with multiple substitutions (Table 3).

## 2.2. Structure–activity relationship in an in vitro cholesterol efflux assay

ApoA-I<sub>cons</sub> analog peptides with single substitutions were tested for their ability to promote cholesterol efflux from macrophages in an in vitro assay (Table 2). As a negative control, we used the apoA-I<sub>cons</sub> peptide (compound **1**) which had been shown to be inactive in the cholesterol efflux assay.<sup>18</sup> As positive controls, we used the HDL peptide mimetics, D4F (**2**) and 5A (**3**) previously reported by others to induce cholesterol efflux.<sup>11,12</sup> In our assay D4F (**2**) and 5A (**3**) exhibited an EC<sub>50</sub> of 2  $\mu$ M  $\pm$  0.25  $\mu$ M and 3.4  $\mu$ M  $\pm$  1.06  $\mu$ M, respectively. As a reference we used purified human apoA-I protein (**4**), which had an EC<sub>50</sub> of 0.1  $\mu$ M. We first tested the apoA-I<sub>cons</sub> analogs (**5–14**) in which a single C6 carbon chain amino acid, S<sub>6H</sub>, of *S* configuration (Fig. 2), was introduced at position 2, 3, 6, 9, 10, 13, 14, 17, 20, or 21, following the scheme in Table 1. These positions are all located on the hydrophobic face of the peptide helical sequence (Fig. 1). Of these analogs, only three exhibited any cholesterol efflux activity: analog S<sub>6H</sub>-13 (**10**), with the substitution at position 13, had an EC<sub>50</sub> of 1.4  $\mu$ M. Analog S<sub>6H</sub>-20 (**13**), with the substitution at position 20, had an EC<sub>50</sub> of 213  $\mu$ M, while analog S<sub>6H</sub>-2 (**5**), with the substitution at position 2, exhibited weak activity only at 100  $\mu$ M, the highest concentration used. We then tested the apoA-I<sub>cons</sub> analogs (**15–24**) in which a single C6 carbon chain amino acid, R<sub>6H</sub>, (Fig. 2) having an opposite configuration with respect to S<sub>6H</sub>, was introduced at hydrophobic positions. Analog R<sub>6H</sub>-13 (**20**), with the substitution at position 13, had an EC<sub>50</sub> of about 31  $\mu$ M, while analogs R<sub>6H</sub>-2 (**15**) and R<sub>6H</sub>-20 (**23**) exhibited weak activity at 100  $\mu$ M. Thus, introduction of both S<sub>6H</sub> and R<sub>6H</sub> at position 13 confers relatively potent cholesterol efflux activity, although the *S* configuration seems to be preferred. If a shorter amino acid side chain (C5) was used, R<sub>5H</sub>-2 (**25**) and R<sub>5H</sub>-13 (**26**), no activity was observed in the cholesterol efflux assay.

Substitution by amino acids with a 7 carbon chain, S<sub>7H</sub>, (analogs **27–33**) confirmed the observation that introduction of an aliphatic amino acid at position 13 confers potent cholesterol efflux capacity on the inactive peptide. Analog S<sub>7H</sub>-13, (**30**), exhibited activity in the cholesterol efflux assay, with potency in a range similar to that

**Table 3**  
In vitro cholesterol efflux from macrophages of apoA-I<sub>cons</sub> mutants obtained by introduction of two or more aliphatic non-natural amino acids at specific positions of the sequence

Compd No. (L-no)	Name	Chol. efflux (EC <sub>50</sub> , $\mu$ M)
46	R <sub>6H</sub> -6/S <sub>7H</sub> -13	0.8 $\pm$ 0.2
47	S <sub>7H</sub> -2/S <sub>7H</sub> -13	0.4 $\pm$ 0.2
48	S <sub>7H</sub> -6/S <sub>7H</sub> -13	0.4 $\pm$ 0.1
49	S <sub>7H</sub> -13/S <sub>7H</sub> -20	0.9 $\pm$ 0.3
50	S <sub>7H3</sub> -6/S <sub>7H3</sub> -13	0.3 $\pm$ 0.2
51	S <sub>8H</sub> -6/S <sub>8H</sub> -13	0.4 $\pm$ 0.3
52	S <sub>8H3</sub> -6/S <sub>8H3</sub> -13	0.6 $\pm$ 0.2
53	S <sub>7H</sub> -6/S <sub>7H</sub> -13, S <sub>7H</sub> -20	1.8 $\pm$ 0.3
54	S <sub>7H</sub> -2/S <sub>7H</sub> -13/S <sub>7H</sub> -20	5 $\pm$ 2
55	S <sub>7H</sub> -2/S <sub>7H</sub> -6/S <sub>7H</sub> -13	1.9 $\pm$ 0.9
56	R <sub>7H</sub> -6/S <sub>7H</sub> -13/S <sub>7H</sub> -20	1.0 $\pm$ 0.5
57	S <sub>7H</sub> -2/R <sub>7H</sub> -6/S <sub>7H</sub> -13	0.9 $\pm$ 0.2
58	S <sub>7H</sub> -2/S <sub>7H</sub> -6/S <sub>7H</sub> -13/S <sub>7H</sub> -20	6.7 $\pm$ 4.6

observed with analog  $S_{6H}$ -13 (**10**). Weak activity was observed with analogs  $S_{7H}$ -6 (**27**) and  $S_{7H}$ -20 (**33**) when tested at a concentration of 100  $\mu$ M. Further, when analogs with single  $R_{7H}$  substitutions (**34–42**) were tested, only the variant with a substitution at position 13,  $R_{7H}$ -13 (**38**), showed significant activity. Substitutions with a non-natural amino acid having an even longer (C8) carbon alkenyl side chain resulted in analog  $S_{8H}$ -13 (**44**), which displayed significantly increased activity ( $EC_{50}$   $0.7 \pm 0.35$   $\mu$ M).

Introduction of fully saturated non-natural amino acids  $S_{7H3}$  (C7 chain) and  $S_{8H3}$  (C8 chain) (Fig. 2) at position 13 resulted in analogs  $S_{7H3}$ -13 (**43**) and  $S_{8H3}$ -13 (**45**), which had potencies  $0.7 \pm 0.08$   $\mu$ M and  $0.7 \pm 0.23$   $\mu$ M, respectively, slightly better than alkenyl mutant  $S_{7H}$ -13 (**30**) but in a similar range with alkenyl mutant  $S_{8H}$ -13 (**44**).

In summary, analysis of the single substitution analogs in the *in vitro* cholesterol efflux assay indicate that activity was gained mainly by the introduction of an aliphatic chain longer than C6 at position 13. Weak activity was also generated by the introduction of an aliphatic chain longer than C6 at positions 2, 6, and 20. Interestingly, if positions 2, 6, 13, 20 are highlighted on the helical wheel representation of the apoA-I<sub>cons</sub> they are all localized on a narrow corridor of the hydrophobic portion along the amphipathic helix (Fig. 1). To determine if cholesterol efflux activity could be further improved with multiple substitutions we synthesized analogs with substitutions at position 13 and at positions 2, 6, or 20. Activity of the double substitution analogs in the cholesterol efflux assay is shown in Table 3. In general, combining a substitution at position 13 with one at any of positions 2, 6, or 20 improved the cholesterol efflux activity of the singly substituted peptide. Introduction of the aliphatic amino acid  $S_{7H}$  at positions 2 and 13 (analog **47**) or positions 6 and 13 (analog **48**) brought an improvement in potency, in the range of 0.4  $\mu$ M, with respect to the potency shown by the single mutant analog having  $S_{7H}$  at position 13 (**30**). Also analogs **47** and **48** were more potent than the singly substituted analog **30** but showed a potency in the same range of single mutants at position 13 with a saturated side chain (**43**) or a longer (C8) carbon chain (**44**, **45**). The double mutant with  $S_{7H}$ , at positions 13 and 20 (analog **49**) seemed to be less potent, with an  $EC_{50}$  near the micromolar range. Similarly, the double mutant previously described<sup>18</sup> with  $R_{6H}$  at position 6 and  $S_{7H}$  at position 13 (**46**) showed a slightly lower potency suggesting that the S configuration was overall preferred.

Introduction of aliphatic amino acids at more than two positions was detrimental for activity in the cholesterol efflux assay, as shown by peptides **53–58** in Table 3. When an analog with a substitution at position 13 was combined with those at 2, 6, or

20 in many possible combinations, either with triple substitutions (**53–57**), or with quadruple substitutions (**58**), all exhibited reduced potency when compared with their respective double substitution analogs.

### 2.3. *In vitro* evaluation of pre- $\beta$ HDL formation

Selected apoA-I<sub>cons</sub> analogs which had shown activity in the *in vitro* cholesterol efflux assay were further characterized for their ability to induce pre- $\beta$  HDL formation upon incubation with plasma. When using human plasma, all peptides tested (**43**, **44**, **45**, **46**, **48**, and **56**) were capable of generating a dose-dependent increase in pre- $\beta$  HDL, with peptide **48** being the most potent among peptides examined (Fig. 3a). In an independent experiment peptides **44**, **46** and **48** were compared with control peptides **1** (apoA-I<sub>cons</sub>) and **2** (D4F) (Supplementary Fig. 1). As expected peptide **1** was completely inactive while peptide **48** was more potent than D4F (**2**), **44** and **46**. Note that the stack-ranking of peptides' potency in pre- $\beta$  HDL formation is slightly different from their stack-ranking in the cholesterol efflux assay. One possible explanation is that the two assays reflect distinct features of the peptides. Reports in the literature suggest that apoA-I mimetic peptides induce formation of pre- $\beta$  HDL by displacing apoA-I from mature HDL.<sup>19</sup> Thus, pre- $\beta$  HDL formation reveals how readily a peptide interacts with mature HDL and subsequently displaces apoA-I, while the cholesterol efflux assay primarily assesses a peptide's ability to interact with the cell membrane and elicit efflux of free cholesterol. Given that peptide **48** appeared to be the most potent peptide in both assays, the two features may be related and collectively determine a peptide's therapeutic potential.

We next examined whether peptide **48** was able to elicit pre- $\beta$  HDL formation upon incubation with mouse plasma. In normal mice the majority of circulating HDL exists in the mature,  $\alpha$ -migrating form (larger than 8.2 nm), with very low levels of pre- $\beta$  HDL present in the 7.1–8.2 nm range.<sup>20–22</sup> Incubation of mouse plasma with increasing concentrations of peptide **48** resulted in a dose-dependent increase in the intensity of the pre- $\beta$  band (Fig. 3b), suggesting that the peptide displaced mouse apoA-I from mature HDL to form pre- $\beta$  particles. Similar observations were reported with peptides **46**<sup>18</sup> and D4F (**2**).<sup>12</sup>

Wool et al. have reported that the apoA-I mimetic L4F (the L-amino acid version of D4F), upon incubation with plasma, localizes mainly within the HDL fraction, although in the presence of isolated LDL, it associates with this lipoprotein.<sup>23</sup> Peptide **48** was incubated with either human or mouse plasma for 2 h. Plasma

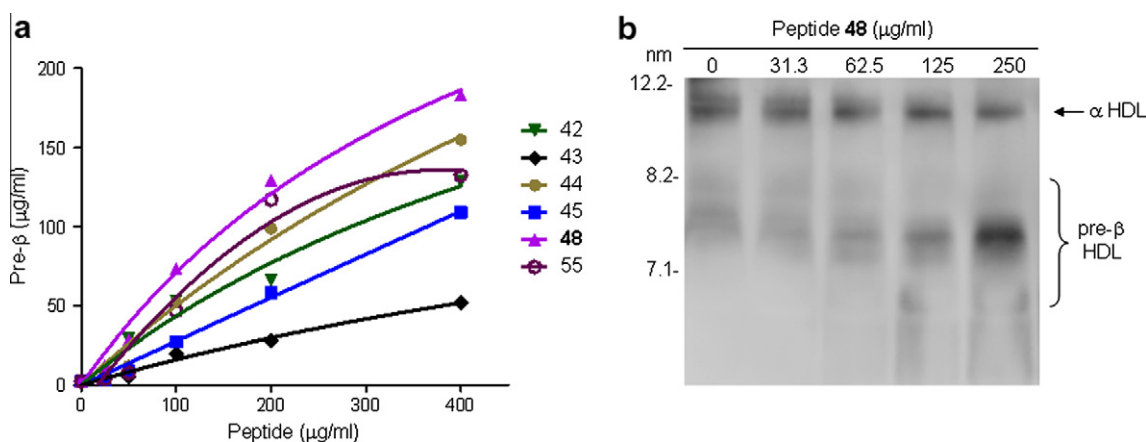


**Figure 3.** (a) Increasing concentrations of selected apoA-I mimetic peptides were incubated with human plasma at 37 °C for 2 h. Pre- $\beta$  HDL formation was assessed by quantitative ELISA. (b) Increasing concentrations of peptide **48** were incubated with C57Bl/6 mouse plasma at 37 °C for 2 h. Pre- $\beta$  HDL formation was assessed by native Western blot. Mature,  $\alpha$  HDL and pre- $\beta$  HDL were identified based on electrophoretic migration.

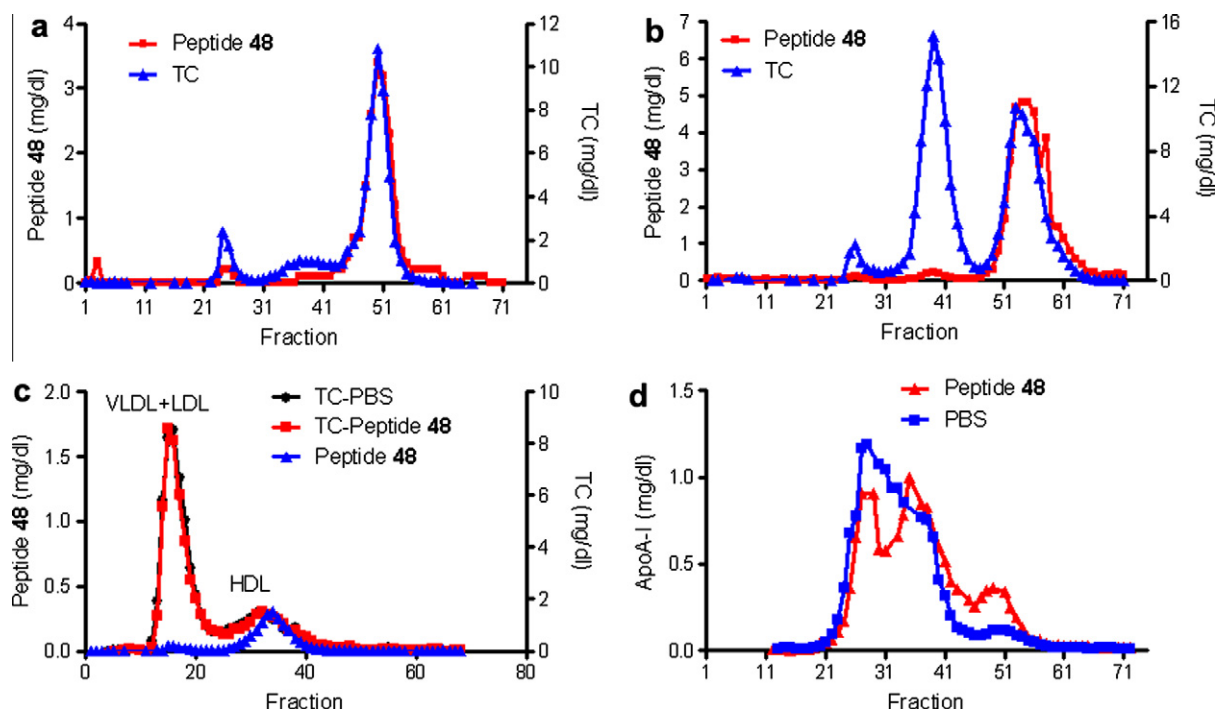


**Figure 4.** (a) Peptide **48** (0.25 mg/ml) was incubated with C57Bl/6 mouse plasma at 37 °C for 2 h, and then subjected to lipoprotein analysis by FPLC. (b) Peptide **48** (0.5 mg/ml) was incubated with human plasma at 37 °C for 2 h, and then subjected to lipoprotein analysis by FPLC. (c) Peptide **48**-treated human plasma was alternatively analyzed by tandem size exclusion chromatography, to allow separation of pre- $\beta$  fractions from mature  $\alpha$ -HDL. Cholesterol and peptide concentrations were measured in resulting fractions. (d) ApoA-I concentrations in resulting fractions were determined using an in-house human apoA-I ELISA.

lipoproteins were then fractionated by size exclusion chromatography, and each fraction was analyzed for cholesterol and peptide content. As shown in Figure 4a and b, peptide **48** preferentially associated with HDL, regardless of the presence or abundance of other lipoproteins. These results suggested that, *in vitro*, peptide **48** has a higher affinity for HDL than LDL or VLDL. Peptide incorporation did not change cholesterol levels in VLDL+LDL, or in HDL (Fig. 4c). Analysis of apoA-I content in the fractions indicated that in control samples (human plasma incubated with PBS) apoA-I appeared as a large peak in fractions containing mature HDL and only as a small peak in fractions containing pre- $\beta$  HDL (Fig. 4d). In comparison, peptide incorporation into mature HDL resulted in an increase in apoA-I in pre- $\beta$  HDL containing fractions (Fig. 4d). These observations confirmed that under the conditions tested, peptide **48** was able to incorporate into mature HDL, while displacing apoA-I to form pre- $\beta$  HDL.

#### 2.4. In vivo evaluation of pre- $\beta$ HDL formation and serum cholesterol efflux

As *in vitro* incubation of peptide **48** with human or mouse plasma resulted in the formation of pre- $\beta$  HDL particles, we proceeded to assess whether a similar phenomenon would occur *in vivo*. Pilot studies in C57Bl/6 mice indicated that administration of peptide **48** to mice, at doses resulting in plasma levels comparable to the concentration of peptide that promoted pre- $\beta$  HDL formation *in vitro*, induced a time- and dose-dependent accumulation of pre- $\beta$  HDL in plasma (data not shown). In order to determine if HDL mimetic peptides would elicit a similar response in a relevant disease model, we tested the ability of peptide **48** to induce pre- $\beta$  HDL formation in *apoe*<sup>-/-</sup> mice. Administration of peptide **48** (60 mg/kg, subcutaneously) to *apoe*<sup>-/-</sup> mice resulted in a time-dependent increase in circulating pre- $\beta$  HDL (Fig. 5a). Pre- $\beta$  HDL is the main acceptor of cellular cholesterol efflux mediated by the ABCA1 transporter.<sup>24</sup> To determine if the pre- $\beta$  HDL induced by the

peptide is active, serum samples from treated animals were used to measure *ex vivo* cholesterol efflux. Cholesterol efflux capacity was increased in the serum harvested from peptide-treated mice. This increase was time-dependent and correlated with an increase in serum pre- $\beta$  HDL (Fig. 5b). Peptide concentration in serum also correlated with both pre- $\beta$  HDL level and cholesterol efflux capacity. Taken together, these results suggest that peptide administration to *apoe*<sup>-/-</sup> mice had triggered HDL remodeling and pre- $\beta$  HDL formation in a fashion similar to that observed in our *in vitro* studies, and that the increase in pre- $\beta$  HDL was likely the main contributor to the increased ABCA1-dependent efflux capacity of the serum samples.

These results indicate that peptide **48** possesses several of the noted beneficial attributes of other apoA-I mimetic peptides, namely the ability to generate pre- $\beta$  HDL formation *in vivo* and to increase serum cholesterol efflux capacity, which is an important pharmacodynamic readout for apoA-I mimetic peptides.

However, we observed no increase in HDL cholesterol, at any peptide dose, either *in vitro* or *in vivo*. As epidemiological observations point to an inverse relationship between plasma HDL-C concentration and cardiovascular risk,<sup>25</sup> the inability of these peptides to increase plasma HDL-C suggests the possibility that they may not have a therapeutic effect.

#### 2.5. Effects of apoA-I mimetic peptides on serum triglyceride levels

Studies in which full length apoA-I was administered to humans, either as lipid-free protein or formulated with diverse phospholipids, showed elevations in circulating triglycerides which paralleled the exposure to exogenous apoA-I.<sup>26–28</sup> A similar observation has been made in mice, rats, and rabbits.<sup>29–31</sup> It has been suggested that apoA-I can induce hypertriglyceridemia by inhibition of the degradation of triglyceride-rich lipoproteins.<sup>26</sup> These observations prompted us to examine the effects of our peptides

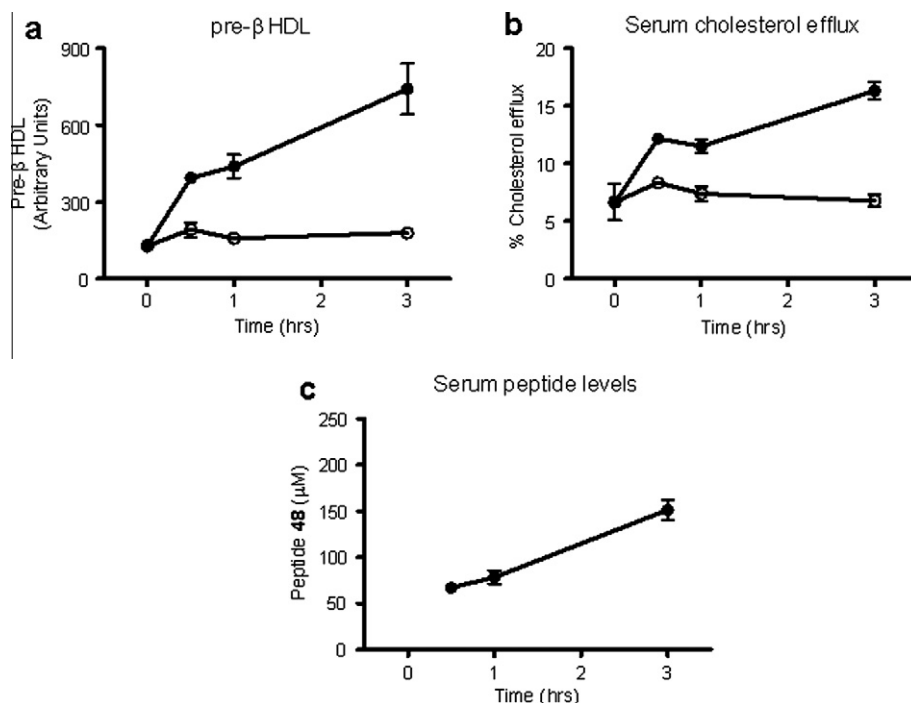


**Figure 5.** (a) Peptide **48** was administered to *apoE*<sup>-/-</sup> mice subcutaneously at 60 mg/kg. Serum samples were collected at various time points post-dosing and analyzed for pre-β HDL formation. (b) ABCA1-dependent cholesterol efflux capacity of the corresponding serum samples was measured in a J774 cholesterol efflux assay. (c) Peptide concentrations in the serum samples.

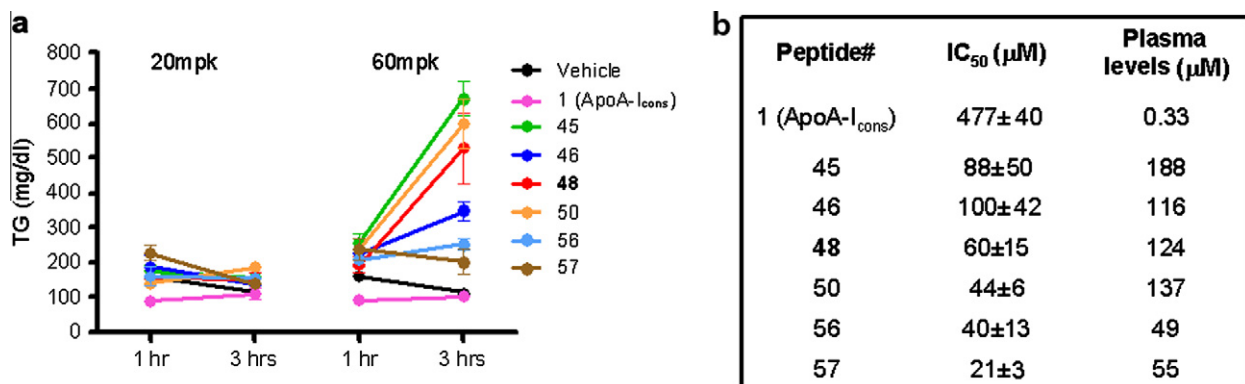


**Figure 6.** (a) Selected peptides were administered to C57Bl/6 mice at 20 or 60 mg/kg subcutaneously. Circulating triglyceride levels in serum samples at 1 or 3 h post-dosing were determined. (b) The same peptides shown in panel 6a were tested for their ability to inhibit LPL activity in vitro. Peptide levels in plasma in panel 6a (60 mg/kg, 3 h) were at or above the IC<sub>50</sub> for LPL inhibition.

on circulating triglyceride levels in mice. As shown in Figure 6a, administration of 20 mg/kg of selected apoA-I mimetic peptides to C57Bl/6 mice had no effect on triglyceride levels, at 1 or 3 h post-administration (the time points where we observed maximal production of pre-β HDL). In contrast, with the exception of peptide **1** (apoA-I<sub>cons</sub>), administration of 60 mg/kg of the same peptides resulted in time-dependent accumulation of triglycerides. Further investigation of this observation indicated that apoA-I mimetic peptides can inhibit lipoprotein lipase (LPL) in an in vitro LPL activity assay (Fig. 6b). All of the peptides tested were capable of inhibiting LPL, but the least potent of them was peptide **1** (apoA-I<sub>cons</sub>). Except for control peptide **1** (apoA-I<sub>cons</sub>), plasma levels for the peptides in the study described in Figure 6a were at or above the IC<sub>50</sub> values of in vitro LPL inhibition, suggesting that triglyceride accumulation in vivo may have resulted from LPL inhibition. Similarly, in an independent experiment, we found that administration of D4F (**2**) and 5A (**3**) at 60 mg/kg, but not at 20 mg/kg, re-

sulted in a time-dependent accumulation of triglycerides (Fig. 2s in Supplementary data). Both D4F and 5A were also capable of inhibiting LPL with an IC<sub>50</sub> of 24 μM ± 3 and 57 μM ± 32, respectively, in the same concentration range of the other peptides tested, suggesting that this might be a class effect and not a specific feature of our apoA-I mimetics.

To further investigate the phenomenon of hypertriglyceridemia, we studied the effects of peptide **48** on lipoprotein composition after administration to C57Bl/6 mice. As shown in Figure 7, administration of peptide **48** at 30 mg/kg (a dose that did not induce hypertriglyceridemia) resulted in a distribution profile in which the peptide associated mostly with HDL, with peak values observed at 3 h (corresponding approximately to the C<sub>max</sub> of the peptide). The accumulation of peptide **48** in the HDL fraction did not induce any significant changes in either cholesterol or triglyceride content of HDL, LDL or VLDL. In comparison, when peptide **48** was dosed at 100 mg/kg, significant hypertriglyceridemia was observed

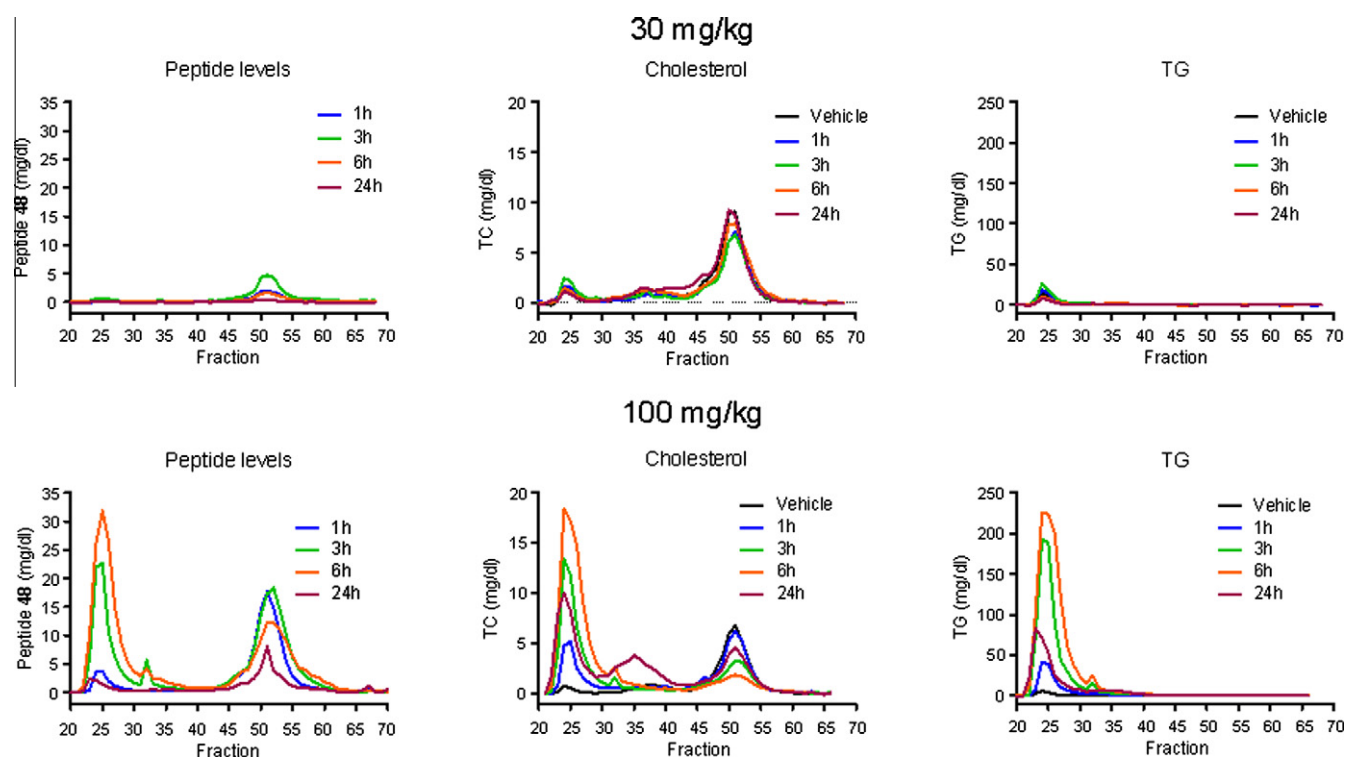


**Figure 7.** Peptide **48** was administered to C57Bl/6 mice at 30 or 100 mg/kg subcutaneously. Serum samples at various time points post-dosing were subjected to lipoprotein fractionation by FPLC. Peptide concentration, cholesterol, and triglyceride levels were determined in resulting fractions.

and the distribution profile of the peptide differed significantly from that observed after a 30 mg/kg dose. We found that although at 1 h the majority of the peptide was associated with HDL, by 3 h there was no observable increase of peptide in the HDL fraction, with all new peptide accumulating in the VLDL fraction. Peptide continued to accumulate in the VLDL fraction up to 6 h. We also observed increases in both cholesterol and triglycerides in VLDL, concurrent with peptide accumulation in VLDL. Triglyceride content of HDL did not change over the 24 h of the study, but HDL cholesterol was surprisingly reduced in parallel with the increase in VLDL cholesterol. At 24 h, we detected an increase in cholesterol in the fractions corresponding to LDL, which could be explained by catabolism of VLDL after clearance of peptide **48**. A similar observation of increased cholesterol content in the VLDL and LDL fractions has been reported by Shah et al. after administration of recombinant human apoA-I<sub>Milano</sub> to *apoE*<sup>-/-</sup> mice.<sup>32</sup> Taken together, these observations suggest that the association of apoA-I mimetic peptide with HDL is likely a saturable process, and that once maximal association is reached, peptide becomes available for association with other lipoproteins, in this case VLDL. Given the ability of apoA-I mimetic peptides to inhibit LPL activity, this initiates a cycle in which VLDL triglycerides accumulate, and this lipoprotein becomes available for the incorporation of any cholesterol the peptide may mobilize.

Thus, special attention has to be paid to the dosing regimen of apoA-I mimetic peptides, and an appropriate therapeutic window needs to be identified to ensure HDL association is not saturated, and there is no surplus of peptide available to interact with VLDL thereby inducing hypertriglyceridemia.

### 3. Conclusions

Our structure–activity relationship studies led us to the identification of potent apoA-I peptide mimetics based on a 22-mer pep-

tide sequence into which non-natural amino acids were introduced at specific positions of the hydrophobic portion. In vitro our mimetics can stimulate cholesterol efflux from macrophages and promote pre- $\beta$  HDL formation in both mouse and human plasma. Their potencies in these activities are superior to other peptide mimetics in development and are in a similar range as apoA-I. When incubated at moderate concentrations with human plasma our peptides are distributed mostly in HDL fractions. When administered to mice, our peptides trigger HDL remodeling and pre- $\beta$  HDL formation. Moreover we observed a concomitant increase in ABCA1-dependent efflux capacity of serum from peptide-dosed animals.

However, regarding therapeutic potential of apoA-I mimetics, there are some concerns. The administration at higher dose of apoA-I mimetics in our study, including previously reported D4F and 5A, resulted in triglyceride accumulation due to LPL inhibition. In fact once our peptides saturated HDL, they incorporated into VLDL and increased plasma triglyceride associated with VLDL. Previous reports about triglycerides elevations with apoA-I protein and our data with D4F and 5A suggest that this might be a class issue. Therefore a narrow therapeutic window in terms of safe dosing might exist for apoA-I peptide mimetics.

## 4. Experimental section

### 4.1. Materials

All amino acid derivatives, the Rink linker *p*-[(R,S)- $\alpha$ -[9H-Fluoren-9-yl-methoxyformamido]-2,4-dimethoxybenzyl]-phenoxyacetic acid, and coupling reagents were purchased from EMD Biosciences. The Fmoc-Linker AM-PS based resin 1% cross-linked was purchased from Biosearch Technologies Inc.

ACS grade solvents were purchased from Sigma–Aldrich (Germany) and used as obtained.

Determination of total cholesterol, triglycerides and fatty acids was performed by colorimetric assays purchased from WAKO Diagnostics (WAKO Chemicals, USA, Inc., Richmond, VA).

[<sup>3</sup>H] cholesterol was purchased from Perkin–Elmer (Waltham, MA). 8-(4-chlorophenylthio)-adenosine 3':5'-cyclic monophosphate (cpt)-cAMP, Bovine serum albumin (BSA), Tris, HEPES (and other buffer reagents), bovine lipoprotein lipase, protease inhibitor cocktail, lipase inhibitors (paraoxon, di-ethyl-*p*-nitrophenyl phosphate) were obtained from Sigma (Sigma–Aldrich, St. Louis, MO). Culture medium (DMEM and others) and fetal calf serum (FCS) were purchased from Invitrogen (Invitrogen Corporation, Carlsbad, CA).

Human pre-β HDL Elisa was obtained from Daiichi (Daiichi Pure Chemicals, Tokyo, Japan). Purified human apoA-I protein, Rabbit anti-mouse apoA-I antibody and monoclonal mouse anti-human apoA-I antibody were purchased from Biodesign International (Saco, ME); HRP-conjugated goat anti-rabbit secondary antibody was purchased from Pierce (Rockford, IL); anti-human apoA-I polyclonal antibody was purchased from Academy Biomedical (Houston, TX). Purified human VLDL was obtained from Intracel (Frederick, MD). Immulon high-binding plates were purchased from ThermoLabsystems.

#### 4.2. Synthesis of non coded hydrocarbon side chain amino acids

The Fmoc hydrocarbon side chain amino acids S<sub>6H</sub>, R<sub>7H</sub>, and S<sub>8H</sub> were synthesized following the same synthetic procedure as previously reported.<sup>18</sup>

##### 4.2.1. Fmoc-S<sub>6H</sub>-OH-(2R)-2-[(9H-fluoren-9-ylmethoxy)-carbonyl]amino]oct-7-enoic acid

Obtained after lyophilization as white powder (54% yield); <sup>1</sup>H NMR (400 MHz, DMSO-*d*<sub>6</sub>) δ: 7.92 (d, 2H), 7.76 (d, 2H), 7.55 (d, 1H), 7.45 (t, 2H), 7.32 (m, 2H), 5.82 (m, 1H), 5.01 (m, 2H), 4.30 (m, 3H), 3.94 (m, 1H), 2.05 (m, 2 H); 1.8–1.6 (m, 2H), 1.38 (m, 4H). MS (ES) C<sub>23</sub>H<sub>25</sub>NO<sub>4</sub> required 379.44, found: 380.4.

##### 4.2.2. Fmoc-R<sub>7H</sub>-OH-(2S)-2-[(9H-fluoren-9-ylmethoxy)-carbonyl]amino]non-8-enoic acid

Obtained after lyophilization as white powder (40% yield); <sup>1</sup>H NMR (400 MHz, DMSO-*d*<sub>6</sub>) δ: 7.96 (d, 2H), 7.75 (d, 2H), 7.65 (d, 1H), 7.45 (t, 2H), 7.32 (t, 2H), 5.84 (m, 1H), 5.01 (m, 2H), 4.42 (m, 3H), 3.94 (m, 1H), 2.04 (m, 2H); 1.65 (m, 2H), 1.36 (m, 6H). MS (ES) C<sub>24</sub>H<sub>27</sub>NO<sub>4</sub> required 393.48, found: 394.4. (>95% ee as revealed by HPLC analysis).

##### 4.2.3. Fmoc-S<sub>8H</sub>-OH-(2S)-2-[(9H-fluoren-9-ylmethoxy)-carbonyl]amino]dec-9-enoic acid

Obtained after lyophilization as white powder (42% yield); <sup>1</sup>H NMR (400 MHz, DMSO-*d*<sub>6</sub>) δ: 7.88 (d, 2H), 7.70 (d, 2H), 7.54 (d, 1H), 7.38 (t, 2H), 7.28 (t, 2H), 4.24 (m, 2H), 3.92 (m, 1H); 1.62 (m, 2H), 1.28 (m, 8 H). MS (ES) C<sub>25</sub>H<sub>29</sub>NO<sub>4</sub> required 407.50, found: 408.5.

#### 4.3. Synthesis of Fmoc-S<sub>7H3</sub>-OH, Fmoc-R<sub>7H3</sub>-OH, and Fmoc-S<sub>8H3</sub>-OH

Direct Pd/C-catalyzed hydrogenation of corresponding unsaturated Fmoc-amino acids (Fmoc-S<sub>7H</sub>-OH, Fmoc-R<sub>7H</sub>-OH, and Fmoc-S<sub>8H</sub>-OH)<sup>18</sup> in MeOH gave the all hydrocarbon non-natural amino acids. We used the standard procedure where the mixture of the substrate (500 mg) and 10% Pd/C (70 mg, 0.05 mol %) in MeOH (20 ml) in a round-bottom flask after two vacuum/H<sub>2</sub> cycles to replace air inside with hydrogen, was vigorously stirred at room temperature (ca. 20 °C) under ordinary hydrogen pressure (balloon) for 30 min. The reaction mixture was filtered using a membrane filter

(Millipore, Millex®-LH, 0.45 μm) and the solvent evaporated under reduced pressure. The crude oil is taken in ethyl acetate, washed three times with H<sub>2</sub>O and dried over Na<sub>2</sub>SO<sub>4</sub>. The white solid is washed with petrol ether and dried under vacuum to afford the desired amino acids as determined by <sup>1</sup>H NMR analysis (74% yield):

##### 4.3.1. Fmoc-S<sub>7H3</sub>-OH-(2S)-2-[(9H-fluoren-9-ylmethoxy)-carbonyl]amino]nonanoic acid

Obtained as white solid; <sup>1</sup>H NMR (400 MHz, DMSO-*d*<sub>6</sub>) δ: 7.88 (d, 2H), 7.70 (d, 2H), 7.54 (d, 1H), 7.38 (t, 2H), 7.28 (t, 2H), 4.24 (m, 2H), 3.92 (m, 1H), 1.65 (m, 2H), 1.42–1.18 (m, 10H), 0.82 (m, 3H). MS (ES) C<sub>24</sub>H<sub>29</sub>NO<sub>4</sub> required 395.49, found: 396.5.

##### 4.3.2. Fmoc-R<sub>7H3</sub>-OH-(2R)-2-[(9H-fluoren-9-ylmethoxy)-carbonyl]amino]nonanoic acid

Obtained as white solid; <sup>1</sup>H NMR (400 MHz, DMSO-*d*<sub>6</sub>) δ: 7.90 (d, 2H), 7.72 (d, 2H), 7.56 (d, 1H), 7.40 (t, 2H), 7.28 (t, 2H), 4.26 (m, 2H), 3.88 (m, 1H), 1.60 (m, 2H), 1.42–1.14 (m, 10H), 0.82 (m, 3H). MS (ES) C<sub>24</sub>H<sub>29</sub>NO<sub>4</sub> required 395.49, found: 396.5.

##### 4.3.3. Fmoc-S<sub>8H3</sub>-OH-(2S)-2-[(9H-fluoren-9-ylmethoxy)-carbonyl]amino]decanoic acid

Obtained as white solid; <sup>1</sup>H NMR (400 MHz, DMSO-*d*<sub>6</sub>) δ: 7.88 (d, 2H), 7.72 (d, 2H), 7.58 (d, 1H), 7.42 (t, 2H), 7.32 (t, 2H), 4.28 (m, 2H), 3.90 (m, 1H), 1.62 (m, 2H), 1.40–1.16 (m, 10H), 0.88 (m, 3H). MS (ES) C<sub>25</sub>H<sub>31</sub>NO<sub>4</sub> required 409.5, found: 410.7.

#### 4.4. Peptide synthesis

The apoA-I mimetic peptides were synthesized by solid phase using Fmoc/Bu chemistry on a peptide synthesizer SYMPHONY (Protein Technologies, Inc). All the acylation reactions were performed for 60 min with a five-fold excess of activated amino acid (HBTU/DIEA) over the resin free amino groups following the end of peptide assembly on the synthesizer. The side chain protecting groups were: *tert*-butyl for Asp and Glu; *tert*-butyloxy carbonyl (BOC) for Lys; trityl for Asn and Gln; 2,2,4,6,7-pentamethylidihydrobenzofuran-5-sulfonyl for Arg. The Proline at the N-terminal was introduced as Ac-Proline-OH by using HBTU/DIEA as coupling reagents in DMF. All the non-natural amino acids (R<sub>7H</sub>, S<sub>7H</sub>, R<sub>8H</sub>, S<sub>8H</sub>, S<sub>7H3</sub>, R<sub>7H3</sub>, S<sub>8H3</sub>, R<sub>8H3</sub>) were coupled manually by using HBTU/DIEA as activators and the coupling repeated if necessary. After the coupling the remainder of the synthesis was performed automatically as described above.

At the end of the synthesis, the dry peptide-resins were individually treated with the cleavage mixture, 88% TFA, 5% phenol, 2% triisopropylsilane, and 5% water for 1.5 h at room temperature. In case of peptides containing olefinic-side chain amino acids, the cleavage mixture was composed by 95% TFA and 5% water. Each resin was filtered and the solution was added to cold methyl-*t*-butyl ether in order to precipitate the peptide. After centrifugation, the peptide pellets were washed three times with fresh cold methyl-*t*-butyl ether to remove the organic scavengers. Final pellets were dried, resuspended in H<sub>2</sub>O, 20% acetonitrile, and lyophilized.

Analytical HPLC was performed on a ReproSil-Pur 300 C4 or C18 column (150 × 4.6 mm, 5 μm, 300 Å) (Dr. Maisch GmbH) or ACE C4 or C18 column (150 × 4.6 mm, 3 μm, 300 Å) (CPS Analytica) flow rate 1 ml/min at 45 °C or Acquity UPLC BEH® C18 column (100 × 2.1 mm, 1.7 μm, 130 Å) (Waters) flow rate 0.4 ml/min at 45 °C. Crude peptides were purified by reverse-phase HPLC using preparative Waters Prep LC 4000 System or GX-281 Gilson Trilution LC equipped with a ReproSil-Pur 300 C4 column (250 × 20 mm, 10 μm) (Dr. Maisch GmbH) or RCM Delta-Pak C4 cartridges (40 × 200 mm, 15 μm) or RCM Delta-Pak C18 cartridges (40 × 200 mm, 15 μm) or ACE C18 (250 × 21 mm, 10 μm, 300 Å) (CPS analitica) and using as eluents (A) 0.1% TFA in water and (B)

0.1% TFA in acetonitrile, flow rate 30 or 80 ml/min, respectively. The purified peptides were characterized by electrospray mass spectrometry on a Micromass LCZ platform and/or Acquity SQD Waters.

#### 4.5. Peptide concentration measurement

Fractions collected from chromatography were mixed at 1:3 ratios with an organic solvent (acetonitrile with 0.1% trifluoroacetic acid). A structurally distinct peptide was also added as internal standard. Samples were spined at 2000 rpm for 10 min. Supernatant was taken and subjected to LC–MS analysis of peptide concentration using the RapidFire System (Biotrove, Woburn, MA). Serum levels of peptide were measured by LC–MS/MS after protein precipitation with acetonitrile.

#### 4.6. Lipid analysis

Total cholesterol or triglyceride in serum or column fractions were determined by enzymatic colorimetry by commercially available assays according to manufacturer's instructions (WAKO Diagnostics).

#### 4.7. In vivo administration of peptides

All studies described here were approved by the Merck Research Laboratories (Rahway, NJ) Institutional Animal Care and Use Committee. Male mice C57Bl/6 (Taconic, Germantown, NY) or *apoE*<sup>−/−</sup> (Jackson Laboratory, Bar Harbor, ME), at least 12 weeks of age, were used in these studies. Animals were maintained in environmentally controlled temperature and humidity facilities, with a 12 h light/dark cycle (7:00 am–7:00 pm). All animals were fed standard rodent chow for the duration of the studies. Animals had ad libitum access to food and water.

On the day of the study, mice were injected subcutaneously with either control vehicle (50 mM mannitol in phosphate buffered saline) or test peptides, at 20–100 mg/kg. At predetermined time points, animals were euthanized by CO<sub>2</sub> asphyxiation, and blood collected by cardiac puncture. Blood was allowed to clot for 1 h at room temperature and serum separated by centrifugation at 10,000g for 10 min. Serum samples were immediately frozen at −80 °C for further analysis (serum-mediated cholesterol efflux, pre-β HDL measurement, triglyceride measurement) or filtered through a 0.65 μm filter (Millipore, Billerica, MA), mixed with lipase and protease inhibitors, and used for lipoprotein isolation as described below. 3–5 animals were used per dose and time point.

#### 4.8. In vitro Cholesterol efflux assay

Mouse macrophage cells (RAW 264.7, ATCC, Manassas, VA) were maintained in DMEM medium with 10% FCS and 1% PSG in T225 flasks to a confluency of ~80%. For efflux assays, cells were seeded into 48 well plates at a concentration of  $1 \times 10^5$  cells/0.2 ml/well in the same medium supplemented with [<sup>3</sup>H] cholesterol.

After 24 h, cells were washed once and starved overnight with serum-free medium supplemented with 0.1% lipid-free BSA. Finally, peptides with or without cAMP in serum-free medium were added and incubated for another 24 h.

Subsequently, medium and cell lysate (0.5% Triton X-100 in 1 mM HEPES, pH 7.5) were collected and aliquots were mixed separately with scintillation cocktail and counted. Cholesterol efflux was calculated as the percentage of radioactivity associated with medium over the sum of radioactivity of both medium and lysate. cAMP-dependent cholesterol efflux was determined by the

difference between cholesterol measured in the presence and the absence of cAMP.<sup>33</sup>

#### 4.9. Ex vivo serum cholesterol efflux assay

ABCA1-dependent serum cholesterol efflux assays were performed similarly to previously described.<sup>21</sup> Briefly, J774 macrophages were seeded in 24 well tissue culture plates, labeled with [<sup>3</sup>H] cholesterol for 24 h, then incubated in media containing 0.2% BSA for 18 h to allow cellular cholesterol radiolabel to equilibrate. Incubations with or without 8-(4-chlorophenylthio)-adenosine 3':5'-cyclic monophosphate (cpt)-cAMP were both included. Cells were then washed once, and incubated with acceptor media containing mouse serum diluted to 2% at 37 °C for 4 h. [<sup>3</sup>H] released into the media was compared with total [<sup>3</sup>H] at time zero to determine the percent release of [<sup>3</sup>H]cholesterol (fractional efflux). ABCA1-dependent efflux was derived by subtracting fractional efflux of non-cAMP-treated cells from fractional efflux of cAMP-treated cells.

#### 4.10. Native gel-Western quantitation of mouse pre-β HDL

Two microliters of peptide **48** solutions of increasing concentration were added to 20 μl C57Bl/6 mouse plasma, incubated at 37 °C for 2 h, and then subjected to one-dimensional, non-reducing, anti-mouse apoA-I Western blotting. Briefly, samples were diluted 1:2 with sample buffer (60% sucrose, 0.1% bromophenol blue) and resolved by nondenaturing, non-reducing one-dimensional 4–20% polyacrylamide gel electrophoresis at 50 V for 30 min and 120 V for 3 h. Gels were transferred to nitrocellulose overnight (28 V at 4 °C). After transfer, the membrane was blocked with 0.5% BSA and washed three times with TBST (10 mM Tris, pH 7.4, 150 mM NaCl, and 0.1% Tween 20). Rabbit anti-mouse apoA-I antibody (Bio-design International) and HRP-conjugated goat anti-rabbit secondary antibody were used as the primary and secondary antibodies, respectively. Blots were developed with ECL reagent (GE Healthcare, Piscataway, NJ), and scanned using a Typhoon 9400 Imager (GE Healthcare, Piscataway, NJ). Pre-β HDL was identified based on electrophoretic mobility (7.1–8.2 nm), and the band was quantitated using ImageQuant software, with the results expressed as arbitrary units (AU) representing signal intensity of the band after background subtraction of an equal-sized area.

#### 4.11. ELISA quantitation of human pre-β HDL

Increasing concentrations of various peptides were incubated with normal human plasma at 37 °C for 2 h, as described above. The amount of pre-β HDL in the resulting samples was determined by a commercially available human pre-β HDL ELISA (Daiichi Pure Chemicals, Tokyo, Japan).

#### 4.12. ELISA quantitation of human apoA-I

Human apoA-I concentrations in samples were determined using a sandwich ELISA. Immulon high-binding plates were coated overnight with 0.5 μg/ml monoclonal mouse anti-human apoA-I antibody at 4 °C. Plates were then blocked with TBST (150 mM NaCl, 50 mM Tris, pH 7.5, 0.05% Tween20) supplemented with 1% BSA for 1 h at room temperature, washed with TBST, and then incubated with diluted samples for 2 h at room temperature. Plates were then washed, incubated with 0.5 μg/ml biotinylated goat anti-human apoA-I polyclonal antibody for 1 h at room temperature. After washes, plates were subjected to the Streptavidin/Europium DELFIA detection system (Envision plate reader, model #2103, Perkin–Elmer, Shelton, CT). Purified human apoA-I was used as a standard.

#### 4.13. Peptide-lipoprotein association in vitro

Peptide **48** was mixed with C57Bl/6 mouse plasma at a final concentration of 0.25 mg/ml or with human plasma at a final concentration of 0.5 mg/ml. Plasma was then incubated at 37 °C for 1 h, and lipoprotein particles fractionated by size exclusion chromatography (see below). To measure peptide association with pre- $\beta$  HDL particles, human plasma was incubated with peptide **48** at 0.1 mg/ml, incubated at 37 °C for 1 h, and then pre- $\beta$  HDL was separated from HDL by tandem size exclusion (tandem HP-SEC) chromatography as described below. A PBS-spiked control sample was also included in these studies.

#### 4.14. Lipoprotein analysis by size exclusion chromatography

Plasma or serum lipoproteins were separated by a fast protein liquid chromatography (FPLC) system using a Superose 6 HR column (Amersham Pharmacia Biotech, Piscataway, NJ). The column was equilibrated with PBS (pH 7.4) plus 1 mM EDTA and was run at a flow rate of 0.2 ml/min. The serum samples were pooled (three animals per pool), supplemented with protease inhibitor cocktail (Sigma) and lipase inhibitor (paraoxon, di-ethyl-*p*-nitrophenyl phosphate, Sigma), filtered with 0.65  $\mu$ m microcentrifuge filters, and then 100  $\mu$ l samples were loaded onto the column. Fractions (0.27 ml) were collected and subjected to analyses as described below.

Lipoprotein analysis by tandem HP-SEC. Tandem HP-SEC was performed at ambient temperature using a Superdex 200 HR 10/30 column connected in series to a Superdex 75 HR 10/30 column in the AKTA FPLC system. The column was equilibrated with PBS (pH 7.4) plus 2 mM EDTA and was run at a flow rate of 0.35 ml/min. The serum samples were pooled (three animals per pool), supplemented with protease inhibitor cocktail and lipase inhibitor, filtered with 0.65  $\mu$ m microcentrifuge filters, and then 100  $\mu$ l samples were loaded onto the column. Fractions (0.25 ml) were collected and subjected to lipid/protein analyses as described above.

#### 4.15. LPL inhibition assay

LPL activity was measured as free fatty acids released from VLDL. Assays were carried out in 96-well plates with a 50  $\mu$ l reaction system that includes PBS, 0.1% BSA, 1 U bovine lipoprotein lipase (Sigma), 12.5  $\mu$ g purified human VLDL (Intracel, Frederick, MD), and various amounts of peptides. Reaction mixture was first incubated on ice for 1 h, and then incubated at room temperature for another hour. Free fatty acids generated in the reaction were quantitated in the same plate using a commercially available kit (Wako).

#### Supplementary data

Supplementary data associated with this article can be found, in the online version, at doi:10.1016/j.bmc.2010.09.074.

#### References and notes

- Linsel-Nitschke, A.; Tall, A. R. *Nat. Rev. Drug Disc.* **2005**, *4*, 193.
- Rader, D. J. *J. Clin. Invest.* **2006**, *116*, 3090.
- Wang, X.; Collins, H. L.; Ranalletta, M.; Fuki, I. V.; Billheimer, J. T.; Rothblat, G. H.; Tall, A. R.; Rader, D. J. *J. Clin. Invest.* **2007**, *117*, 2216.
- Wang, N.; Silver, D. L.; Costet, P.; Tall, A. R. *J. Biol. Chem.* **2000**, *275*, 33053.
- Rubin, E. M.; Krauss, R. M.; Spangler, E. A.; Verstuyft, J. G.; Clift, S. M. *Nature* **1991**, *353*, 265.
- Plump, A. S.; Scott, C. J.; Breslow, J. L. *Proc. Natl. Acad. Sci. USA* **1994**, *91*, 9607.
- Nissen, S. E. et al. *JAMA* **2003**, *290*, 2292.
- Tardif, J.-C. *JAMA* **2007**, *297*, 1675.
- Natarajan, P.; Forte, T. M.; Chu, B.; Phillips, M. C.; Oram, J. F.; Bielicki, J. K. *J. Biol. Chem.* **2004**, *279*, 24044.
- Gillotte, K. L.; Zaiou, M.; Lund-Katz, S.; Anantharamaiah, G. M.; Holvoet, P.; Dhoest, A.; Palgunachari, M. N.; Segrest, J. P.; Weisgraber, K. H.; Rothblath, G. H.; Phillips, M. C. *J. Biol. Chem.* **1999**, *274*, 2021.
- Remaley, A. T.; Thomas, F.; Stonik, J. A.; Demosky, S. J.; Bark, S. E.; Neufeld, E. B.; Bocharov, A. V.; Vishnyakova, T. G.; Patterson, A. P.; Eggerman, T. L.; Santamarina-Fojo, S.; Brewer, H. B. *J. Lipid Res.* **2003**, *44*, 828.
- Navab, M.; Anantharamaiah, G. M.; Srinivasa, T. R.; Hama, S.; Hough, G.; Grijalva, V. R.; Wagner, A. C.; Frank, J. S.; Datta, G.; Garber, D.; Fogelman, A.-M. *Circulation* **2004**, *3215*.
- Sethi, A. A.; Stonik, J. A.; Thomas, F.; Demosky, S. J.; Amar, M.; Neufeld, E.; Brewer, H. B.; Davidson, W. S.; D'Souza, W.; Sviridov, D.; Remaley, A. T. *J. Biol. Chem.* **2008**, *283*, 32273.
- Tabet, F.; Remaley, A. T.; Segaliny, A. I.; Millet, J.; Yan, L.; Nakhla, S.; Barter, P. J.; Rye, K.-A.; Lambert, G. *Arterioscler. Thromb. Vasc. Biol.* **2010**, *3*, 246.
- Navab, M.; Anantharamaiah, G. M.; Hama, S.; Garber, D. W.; Chaddha, M.; Hough, G.; Lallone, R.; Fogelman, A. M. *Circulation* **2002**, *105*, 290.
- Li, X.; Chyu, K.-Y.; Faria Neto, J. R.; Yano, J.; Nathwani, N.; Ferreira, C.; Dimayuga, P. C.; Cercek, B.; Kaul, S.; Shah, P. K. *Circulation* **2004**, *110*, 1701.
- Anantharamaiah, G. M.; Venkatachalapathi, Y. V.; Brouillette, C. G.; Segrest, J. P. *Arteriosclerosis* **1990**, *10*, 95.
- Ingenito, R.; Burton, C.; Langella, A.; Chen, X.; Zytka, K.; Pessi, A.; Wang, J.; Bianchi, E. *Bioorg. Med. Chem. Lett.* **2010**, *20*, 236.
- Wool, G. D.; Reardon, C. A.; Getz, G. S. *J. Lipid Res.* **2008**, *49*, 1268.
- Ishida, B. Y.; Frolich, J.; Fielding, C. J. *J. Lipid Res.* **1987**, *28*, 778.
- Duong, P. T.; Weibel, G. L.; Lund-Katz, S.; Rothblat, G. H.; Phillips, M. C. *J. Lipid Res.* **2008**, *49*, 1006.
- Trount, J. S.; Alborn, W. E.; Mosior, M. K.; Dai, J.; Murphy, A. T.; Beyer, T. P.; Zhang, Y.; Cao, G.; Konrad, R. J. *J. Lipid Res.* **2008**, *49*, 581.
- Wool, G. D.; Vaisar, T.; Reardon, C. A.; Getz, G. S. *J. Lipid Res.* **2009**, *50*, 1889.
- Rye, K. A.; Barter, P. J. *Arterioscler. Thromb. Vasc. Biol.* **2004**, *24*, 421.
- Castelli, W. P.; Garrioso, R. J.; Wilson, P. W.; Abbott, R. D.; Kalousdian, S.; Kannel, W. B. *JAMA* **1986**, *256*, 2835.
- Nanjee, M. N.; Crouse, J. R.; King, J. M.; Hovorka, R.; Rees, S. E.; Carson, E. R.; Morgenthaler, J. J.; Lerch, P.; Miller, N. E. *Arterioscler. Thromb. Vasc. Biol.* **1996**, *16*, 1203.
- Nanjee, M. N.; Doran, J. E.; Lerch, P. G.; Miller, N. E. *Arterioscler. Thromb. Vasc. Biol.* **1999**, *19*, 979.
- Shaw, J. A.; Bobik, A.; Murphy, A.; Kanellakis, P.; Blomberg, P.; Mukhamedova, N.; Woollard, K.; Lyon, S.; Sviridov, D.; Dart, A. M. *Circ. Res.* **2008**, *103*, 1084.
- Pedersen, T. X.; Bro, S.; Andersen, M. H.; Etzerodt, M.; Jauhiainen, M.; Moestrup, S.; Nielsen, L. B. *Atherosclerosis* **2009**, *202*, 372.
- Ha, Y. C.; Trifunovic, Z.; Howlett, G. J. *Biochim. Biophys. Acta* **1992**, *1125*, 223.
- Van Lenten, B. J.; Wagner, A. C.; Navab, M.; Anantharamaiah, G. M.; Hama, S.; Reddy, S. T.; Fogelman, A. M. *J. Lipid Res.* **2007**, *48*, 2344.
- Shah, P. K.; Yano, J.; Reyes, O.; Chyu, K. Y.; Kaul, S.; Bisgaier, C. L.; Drake, S.; Cercek, B. *Circulation* **2001**, *103*, 3047.
- Chen, X.; Burton, C.; Song, X.; McNamara, L.; Langella, A.; Cianetti, S.; Chang, C. H.; Wang, J. *Int. J. Biol. Sci.* **2009**, *5*, 489.